30 July 1999

ELSEVIER

Chemical Physics Letters 308 (1999) 428–436

CHEMICAL PHYSICS LETTERS

www.elsevier.nl/locate/cplett

Partial double- and single-differential cross-sections for CO_2 by electron collision

Satyendra Pal

Physics Department, Janta Vedic College (C.C.S. University, Meerut), Baraut 250 611, India

Received 18 September 1998; in final form 28 April 1999

Abstract

This Letter reports the partial double-differential cross-section (PDDCS) and the partial single-differential cross-sections (PSDCS) for the CO_2 molecule by electron collision at 100 and 500 eV. The two direct ionization channels producing CO_2^+ and CO_2^{2+} and the four dissociative channels producing CO^+, C^+, O^+ and C^{2+} are examined. The calculations as a function of energy loss were made by employing a semi-empirical formula which requires the oscillator strengths as input data. For the evaluation of PDDCS with respect to exit electron(s) energy and the scattering angle, the differential generalized oscillator strengths were used in the optical limit. The partial ionization cross-sections (PICS) are also calculated, with electron energies varying from ionization threshold to 10 keV.

1. Introduction

The present work on the CO_2 molecule is in keeping with our thorough and systematic direct and dissociative electroionization study of molecules. Owing to its major importance in many fields, the CO_2 molecule has been investigated by almost all the available spectroscopic techniques [1,2]. Data concerning the electron impact ionization of the CO_2 molecule are of great importance in physics and chemistry of the ionized gases and play an important role in analyzing environmental problems and spacecraft observations of CO emissions from the upper atmosphere of Mars [3].

The total electroionization cross-sections of molecules have been supplemented in recent years by the determination of *N*-fold differential cross-sections [4]. On the other hand, the experimental data for partial ionization cross-sections (PICS) of the CO_2 molecule have been reported by various workers [5–13]. Due to the difficulties in ensuring the complete collection of energetic fragment ions, the accurate measurements of PICS is quite difficult. However, in all the previous measurements of PICS, the data of Freund et al. [12] and Straub et al. [13] are claimed to be absolute. Besides PICS, Shyn and Sharp [14] measured the total double- and total single-differential cross-sections at electron energies varying from 40 to 400 eV, Ogurtsov [15] at electron ejection angle 54.5° in the electron energy range 100–1000 eV and Opal et al. [16] at 500 eV. To the best of our knowledge, no attempt has been made to

0009-2614/99/$ - see front matter
PII: S0009-2614(99)00590-4

measure/calculate the *N*-fold partial differential cross-sections, for example, partial double-differential cross-sections (PDDCS) and partial single-differential cross-sections (PSDCS) for the CO_2 molecule.

On the theoretical side, ab-initio calculations have not yet provided even the PICS for a molecular system. In this context, Jain and Khare have suggested a semi-empirical approach for the conversion of photoionization cross-section data to obtain the electron cross-sections [17]. This semi-empirical formula with necessary modifications has been plucked to evaluate the PSDCS and PICS for molecules [18–20]. Recently, Pal et al. [21] have evaluated the PDDCS for H_2, differential in energy and scattering angle of the ejected electron in a wide range of impinging electron energy. Since the PDDCS are isotropic, the oscillator strengths must be isotropic but it was not considered in our previous calculations for H_2 [21]. The aim of the present work is to modify the oscillator strengths in terms of the cosine distribution form and to produce the partial differential cross-sections for CO_2 in the complete secondary electron energy spectrum, i.e., 0 to (E–I).

To evaluate the PDDCS, triple-differential generalized oscillator strengths (TDGOS) are used in the Bethe regime [22] as input. The calculations are made as a function of energy loss W (the sum of the secondary electron energy ε and the ionization threshold I) suffered by the primary electron or the secondary electron(s) energy (ε) and a scattering angle of 60°. The PSDCS are evaluated as a function of W by the integration of PDDCS over all the solid angle. The incident electron energies used are 100 and 500 eV. Due to the non-availability of experimental data for PDDCS and PSDCS, the total PDDCS (DDCS) and total PSDCS (SDCS) are compared with the experimental data [14–16]. The PICS evaluated in the impinging electron energy range from the ionization threshold to 10 keV show a satisfactory agreement with several experimental data. Notwithstanding, with the dissociative ionization processes, the recent data of Straub et al. [13] (with an absolute uncertainty of 4–10.5%) are in significant disagreement with our results and other experimental data. For direct ionization processes (CO_2^+, CO_2^{2+}), the agreement of the present calculations with Ref. [13] is considerably.

2. Theoretical

Since the modified semi-empirical approach has been described elsewhere (see, e.g., Refs. [18–21]), we will not repeat the details here. Basically, the partial double-differential cross-sections for the production of ith type of ion by the impact of an electron of energy E with a molecule leaving secondary electron(s) of energy ε is given as,

$$Q_i(E,W,\theta) = \left[\frac{a_0^2R^2}{E}\int_{K\to 0}\frac{E-W}{E-I_i}\frac{1}{W}\mathrm{d}f_i(W,K,\theta) \times \ln\left[1+C_i(E-I_i)\right] + \frac{E-I_i}{E\left(\varepsilon_0^3+\varepsilon^3\right)} \times S_i\left(\varepsilon - \frac{\varepsilon^2}{E-\varepsilon} + \frac{\varepsilon^2}{(E-\varepsilon)^2}\right)\right]\sin\theta, \quad (1)$$

where a_0, R, K, S and θ represent the first Bohr radius, Rydberg's constant, momentum transfer, number of ionizable electrons and the scattering angle, respectively. Summation of PDDCS over i gives the total PDDCS (DDCS):

$$Q_i^{\mathrm{T}}(E,W,\theta) = \sum_i Q_i(E,W,\theta). \quad (2)$$

Here it is interesting to note that $Q_i(E,W,\theta)$ is isotropic and hence the material property of molecule, i.e., the oscillator strength must be isotropic in nature. Here $\mathrm{d}f_i(W,K,\theta)$, the differential generalized oscillator strength (DGOS) in the optical limit ($K\to 0$) has been used. From Lassettre's theorem [22], the DGOS in the Bethe regime is reduced to the cosine distribution form of the linear optical oscillator strengths $\mathrm{d}f_i(W,0)/\mathrm{d}W$, i.e.,

$$\mathrm{d}f_i(W,K,\theta) \to (1/4\pi)\left[1+\beta P_2(\cos\theta)\right] \times \mathrm{d}f_i(W,0)/\mathrm{d}W, \quad (3)$$

where β is the asymmetric parameter and $P_2(\cos\theta) = \frac{1}{2}(3\cos^2\theta - 1)$ is the second-order Legendre polynomial. In the present treatment, β is chosen as the probability of ionizing electrons in the ionization process(es), however, it depends on the ejected electron energy. The oscillator strengths are directly

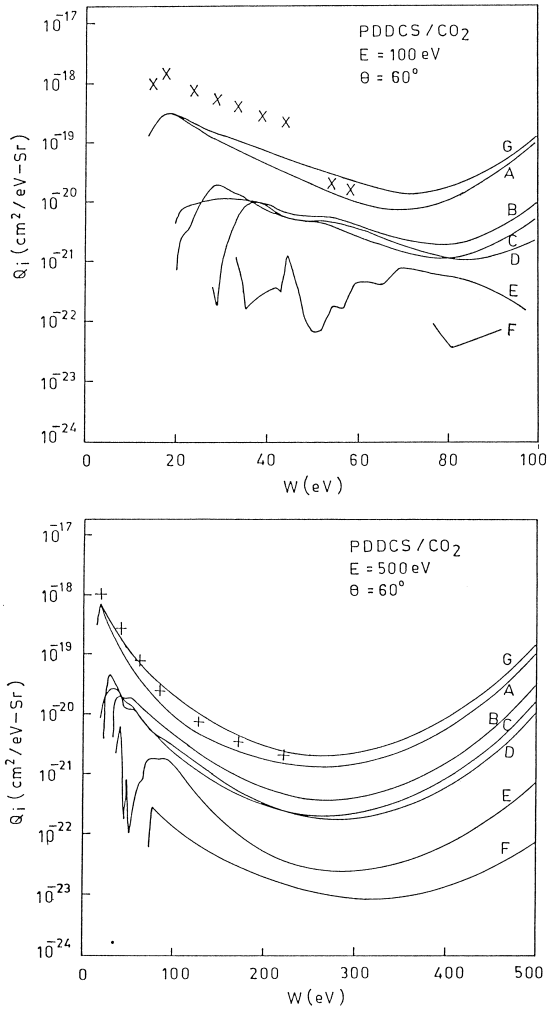

Fig. 1. PDDCS for electroionization of CO_2. Solid curves A, B, C, D, E, F and G correspond to the CO_2^+, O^+, CO^+, C^+, CO_2^{2+} and C^{2+} ions and their sum, respectively, at 100 and 500 eV. Experimental data: ×, Ref. [14] and +, Ref. [16].

proportional to the photo-ionization cross-sections [23]. Further integration of Eq. (1) with respect to the scattering angle θ (from 0 to 2π) gives the PSDCS.

$$Q_i(E,W) = \int Q_i(E,W,\theta)\,\mathrm{d}\Omega\,, \tag{4}$$

where differential solid angle $\mathrm{d}\Omega$ is $2\pi \sin\theta\,\mathrm{d}\theta$. Similarly, SDCS are given as

$$Q_i^{\mathrm{T}}(E,W) = \sum_i Q_i(E,W)\,. \tag{5}$$

Further integration of PSDCS with respect to W from I to $W_{\max}$ $(=E)$, results in PICS, i.e.,

$$Q_i(E) = \int Q_i(E,W)\,\mathrm{d}W\,. \tag{6}$$

The present formulation requires the major input data of the photoionization cross-sections in terms of the optical oscillator strengths. From vertical ionization thresholds to 70 eV, these values for dissociative processes are taken from the compilation of Gallagher et al. (10–15% uncertainty) [23] and for direct

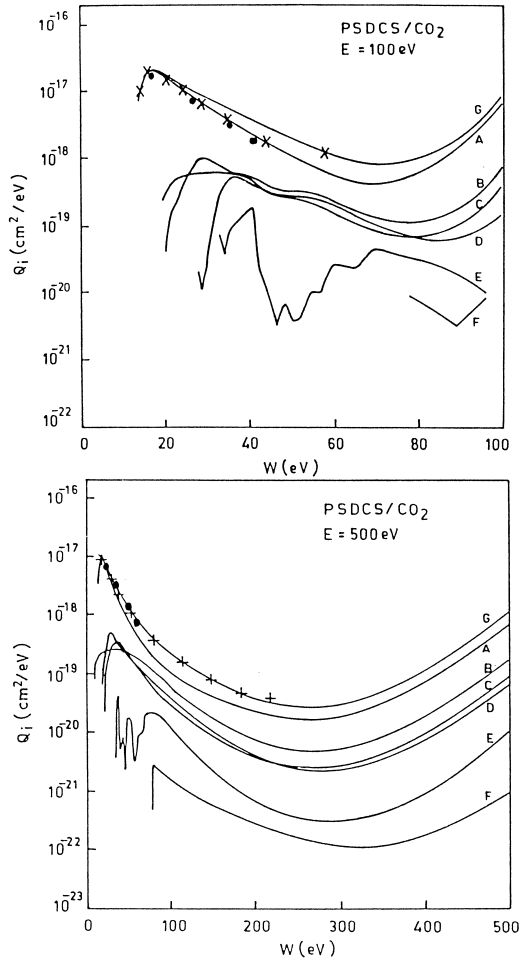

Fig. 2. Same as Fig. 1, but for PSDCS for electroionization of CO_2. Experimental data: ×, Ref. [14]; ●, Ref. [15]; and +, Ref. [16].

ionization processes from Masuoka (> 95% ion collection efficiency) [24]. For higher photon energy ($W > 70$ eV), we have used the total oscillator strength calculated by Zeiss et al. [25], using the additive sum rule. Assuming the ionization efficiency to be unity for $W > 70$ eV, these total oscillator strengths are distributed among the various types of ions for the CO_2 molecules with the help of the branching ratio at breakdown [24]. However, the branching ratio in the measurements is applicable only for the valence-shell orbital. Due to the distribution of total oscillator strengths, the error introduced in the calculations of cross-sections is not expected to be more than the error in the measurement of $df_i(W,0)/dW$. At the present level of calculations, the contribution of K-shell or inner-shell ionization to the Bethe part in the above equations is not more than 3.5% and is thus ignored. Furthermore, if the limit of E is > 1 keV, the relativistic correction is taken into account. The mixing parameter ε_0, assumed to be independent of i, is calculated from the comparison of Bethe and Møller differential cross-sections, i.e., 100 eV [17]. The total collision parameters C_T, calculated from the accurate ($\sim 5\%$) high-energy experimental data of Reike and Prepejchal [26], is used to compute the partial collision parameter $C_i(E)$ which is dependent on both the ionic nature and the energy of the incident electron [18]. For the direct ionization product CO_2^+, where $i = 1$, C_i is nothing but C_T and for $i > 1$, C_i values are found in increasing order with ith values as well as the incident electron energy. Thus the utilization of the partial collision parameter could reduce the deviation by $\sim 4\%$ in the present calculations.

Table 1
Partial double-differential cross-sections (PDDCS) for CO_2

(a) PDDCS (cm^2/eV-Sr) for CO_2 ($E = 100$ eV and $\theta = 60°$)

W (eV)	CO_2^+ ($\times 10^{-20}$)	CO^+ ($\times 10^{-22}$)	O^+ ($\times 10^{-22}$)	C^+ ($\times 10^{-22}$)	CO_2^{2+} ($\times 10^{-22}$)	C^{2+} ($\times 10^{-22}$)	Total ($\times 10^{-20}$)
15	19.7						19.7
20	29.0	24.9	44.2				29.7
30	10.0	185.0	114.0	14.0			13.1
40	4.5	67.3	87.9	82.9			6.9
50	1.9	45.8	56.7	48.8	0.1		3.4
60	1.0	28.2	42.1	38.2	4.4		2.1
70	0.7	15.1	23.4	18.8	7.9		1.3
83	1.3	12.0	20.6	10.5	5.1	1.06	1.7
93	2.4	17.2	29.5	11.3	3.6	0.56	3.0
96	5.9	34.9	60.2	17.8	1.8	0.16	7.0

(b) PDDCS (cm^2/eV-Sr) for CO_2 ($E = 500$ eV and $\theta = 60°$)

W (eV)	CO_2^+ ($\times 10^{-22}$)	CO^+ ($\times 10^{-22}$)	O^+ ($\times 10^{-22}$)	C^+ ($\times 10^{-22}$)	CO_2^{2+} ($\times 10^{-22}$)	C^{2+} ($\times 10^{-22}$)	Total ($\times 10^{-22}$)
15	6950.0						6950.0
20	7800.0	18.5	162.0				7980.0
30	4160.0	783.0	468.0	329.0			5440.0
40	2130.0	324.0	412.0	300.0	0.01		3166.0
50	1020.0	257.0	309.0	206.0	0.02		1792.0
60	575.0	186.0	272.0	194.0	12.40		1240.0
70	365.0	115.0	174.0	119.0	28.90		802.0
96	150.0	44.0	87.3	58.7	31.40	1.64	373.0
160	47.3	9.3	18.6	11.2	2.07	0.63	89.1
200	30.4	5.1	9.8	5.2	0.88	0.38	52.0
300	26.0	3.7	6.8	3.2	0.43	0.15	40.3
400	91.7	12.1	22.3	9.9	1.16	0.23	137.4

Hence, the statistical error in the present calculations for direct and dissociative ionization processes is ~ 8% and 12%, respectively. In the present study, *i*th values from 1 to 6 correspond to the production of the CO_2^+, O^+, CO^+, C^+, CO_2^{2+} and C^{2+} ions, respectively, via direct and dissociative ionization processes of the CO_2 molecule by electron collision.

3. Results and discussion

Figs. 1 and 2 along with Tables 1 and 2 show the present results for PDDCS and PSDCS at 100 and 500 eV with respect to the energy loss function or the secondary electron energy. As mentioned earlier, no previous data exist with which comparison of PDDCS and PSDCS at either energy can be made. To check the accuracy of the present results, we have carried out a comparison of total PDDCS and total PSDCS with the available experimental data [14–16]. In the figures, curves A, B, C, D, E, F and G represent the differential cross-sections for the production of the CO_2^+, O^+, CO^+, C^+, CO_2^{2+}, C^{2+} ions and the total differential cross-sections, respectively, by electron impact CO_2.

Fig. 1 presents the double-differential cross-sections at a scattering angle of 60°. At 100 eV, the present results for DDCS are significantly lower than the experimental data of Shyn and Sharp [14] while at 500 eV, good agreement with the experimental data of Pal et al. [19,20] is observed. In Fig. 2, we note that at 100 eV, the present results for SDCS are ~ 2 times lower than the data [14,15], while at 500 eV, the present results are in satisfactory agreement

Table 2
Partial single-differential cross-sections (PSDCS) for CO_2

(a) PSDCS (cm^2/eV) for CO_2 at $E = 100$ eV

W (eV)	CO_2^+ ($\times 10^{-20}$)	CO^+ ($\times 10^{-20}$)	O^+ ($\times 10^{-20}$)	C^+ ($\times 10^{-20}$)	CO_2^{2+} ($\times 10^{-20}$)	C^{2+} ($\times 10^{-21}$)	Total ($\times 10^{-20}$)
15	2400						240
20	1800	50.0	80.0				1800
30	1140	100.0	201.0	79.6			1241
40	524	56.2	35.4	50.0	4.7		670
50	300	29.5	34.1	27.1	0.6		392
60	185	18.8	26.7	19.6	0.9		251
70	130	11.8	15.3	10.6	3.9		172
80	126	9.4	13.0	6.9	2.7	5.64	159
96	436	23.4	34.3	11.8	5.6	1.42	513

(b) PSDCS (cm^2/eV) for CO_2 at $E = 500$ eV

W (eV)	CO_2^+ ($\times 10^{-20}$)	CO^+ ($\times 10^{-22}$)	O^+ ($\times 10^{-22}$)	C^+ ($\times 10^{-22}$)	CO_2^{2+} ($\times 10^{-22}$)	C^{2+} ($\times 10^{-22}$)	Total ($\times 10^{-20}$)
15	505.0						505.0
20	781.0	134.0	1180.0				794.1
30	302.0	680.0	3400.0	329.0			346.1
40	154.0	2430.0	2990.0	2180.0			230.0
50	74.2	1860.0	2240.0	1500.0	0.1		130.3
60	41.8	1350.0	1970.0	1410.0	89.7		90.0
70	26.5	837.0	1260.0	861.0	210.0		58.2
80	17.6	462.0	851.0	567.0	234.0	24.8	39.0
96	10.9	321.0	634.0	426.0	22.8	15.6	25.1
160	3.9	86.0	178.0	112.0	21.5	5.5	7.9
200	2.2	37.4	71.3	38.5	6.4	2.8	3.8
300	1.9	26.9	49.6	23.2	3.1	1.1	2.9
400	6.7	87.7	162	71.9	8.4	1.6	10.0

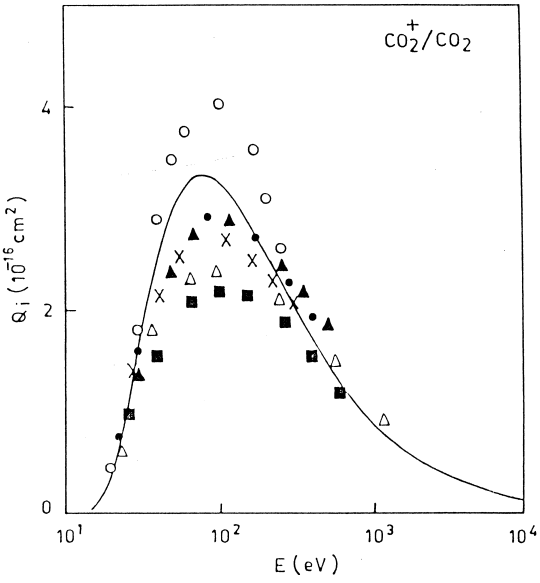

Fig. 3. PICS for the production of CO_2^+. Present results: −. Experimental data: ○, Ref. [6]; ■, Ref. [7]; ×, Ref. [9]; ●, Ref. [10]; ▲, Ref. [11]; and △, Ref. [13].

with the data [15,16]. Further, there is no way to compare the present results above $W > (E + I)/2$, the maximum energy employed in the experiments. However, the present results are symmetric with respect to $W/2$. It is remarkable that differential cross-sections can be divided qualitatively in two parts, one the dipole allowed part, known as the glancing collision and second the nondipole part known as the knock-on collision, corresponding to the Bethe and the Møller parts of the present semi-empirical formula. Large values of the differential cross-sections for slow secondary electrons appear from the growing contribution of the dipole allowed interaction while above $W \geq (E + I)/2$ the cross-section is highly affected by the exchange effects, which are taken into account through the Møller part of the formula. It is also noted that near the threshold ($\varepsilon = 3.0$ eV), the deviation is due to the contribution of autoionization of CO_2, which is not apparent in the various graphs (A and G) in the figures due to its small contribution.

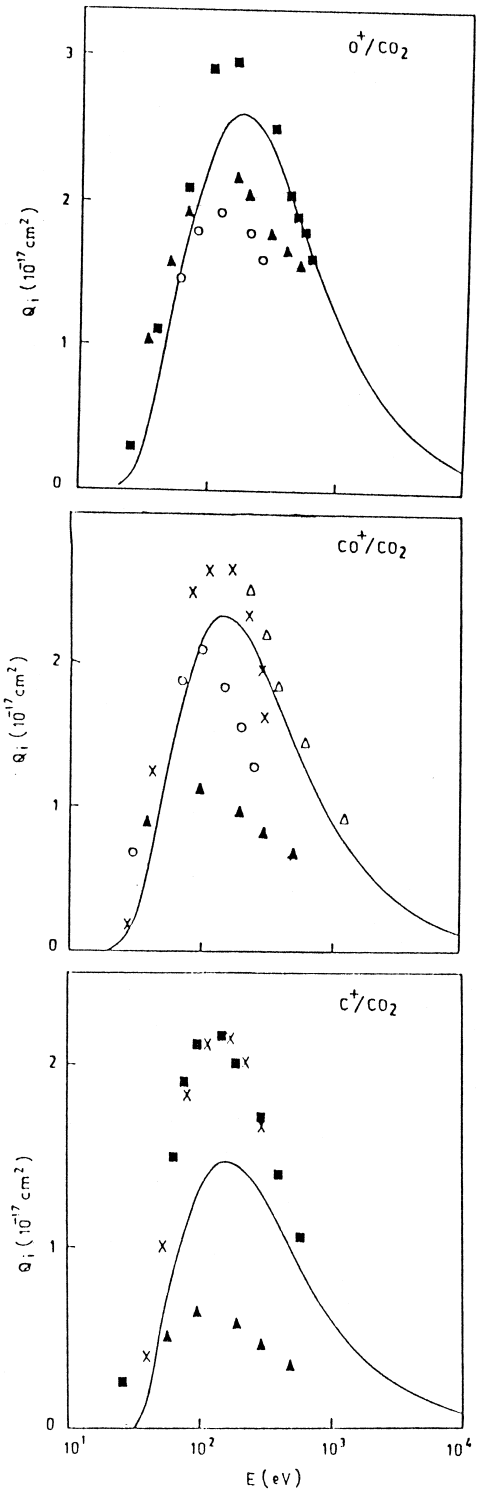

Fig. 4. Same as Fig. 3 but for the production of O^+, CO^+ and C^+ ions.

Figs. 3–5 along with Table 3 show the PICS for the production of various ions through the direct, dissociative and multiple electron ionization of CO_2. In the single ionization, the production of stable CO_2^+ ions is a dominant process throughout the energy region examined, whereas in multiple ionization, dissociation becomes a dominant process because of the strong coulombic repulsion between the two positive holes. For the production of CO_2^+, and multiple CO_2^{n+} ions at high energy, the bond type electronic states of these ions and/or the Rydberg states play an important role through autoionization. In the region of inner valence multiple ionization, the charge localized dissociation of multiple CO^{n+} in terms of minor processes also provides a significant contribution in the cross-sections. The present calculated results for the production of CO_2^+ ions through the direct ionization shown in Fig. 3 are in satisfactory agreement with the experimental data [6,9–12] within the experimental uncertainty. In the energy regime 80–150 eV, the experimental data of Adamczyk et al. [7] are not in agreement with the calculated results, while, in the low-energy range, i.e., near the threshold and above 150 eV, the agreement is fair. On the other hand, the experimental data [5,8,12] are much lower than the present results and other experimental data. Hence, for the sake of clarity and the reasonable shape of the figure, these points are not shown in Fig. 3.

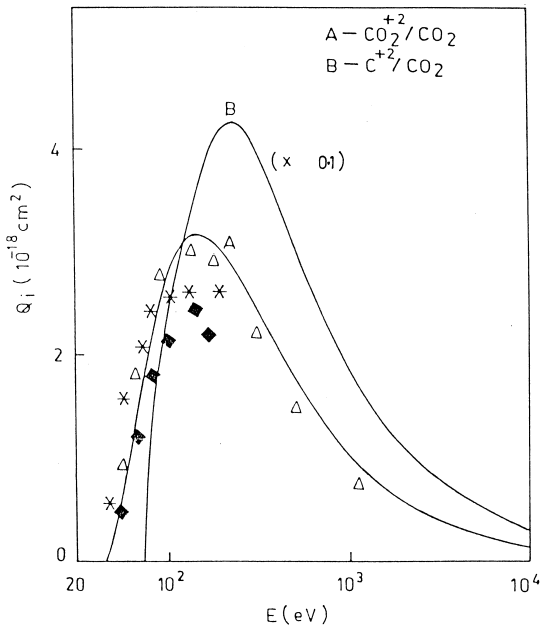

Fig. 5. Same as Fig. 3 but for the production of CO^{+2} and C^{2+} ions via solid curves A and B, respectively. Experimental data: ◆, Ref. [5]; ∗, Ref. [8]; and △, Ref. [13].

Fig. 4 shows the comparison of the calculated dissociative ionization cross-sections for the production of O^+, CO^+ and C^+ ions from the electron impact ionization of the CO_2 molecule with the experimental data [6,7,11]. In the dissociative channels, the production of O^+ is the dominant process (quantitatively) compared to other minor ions, e.g., CO^+, C^+ and C^{2+}. In this figure, we observed a general agreement between our cross-sections for the O^+ ions with the experimental data [7,11]. For the production of the O^+ ions, the experimental data [9] (not shown) lie much lower than the present results and the other experimental data [7,11] too. The present calculations for the CO^+ ions are in satisfactory agreement with the experimental data of Crowe and McConkey [9]. Below 100 eV, the present results are in good agreement with the experimental data of Peresse and Tuffin [6] but above 100 eV the deviation increases rapidly. On the other hand, the experimental data [7,11] are much lower than the present results for CO^+. On the other side, for $E > 200$ eV, the present results for CO^+ show a good agreement with the absolute experimental data [13]. The present results for the C^+ ions are $\sim 25\%$ lower than the experimental data [7,9] and higher by $\sim 40\%$ than the experimental data of Orient and Srivastava [11]. The experimental data [7,13] (not shown) are much higher than the present results.

In Fig. 5, curves A and B represent the production of the CO_2^{2+} and C^{2+} ions, respectively, from the electron impact ionization of the CO_2 molecule. For the CO_2^{2+} ions (curve A), the calculated results are in good agreement with the experimental data [5,8,13] within experimental uncertainty. However, the experimental data of Peresse and Tuffin [6] (not shown) are much lower than the theoretical results and these experimental data points. Furthermore, the experimental data [13] (not shown) are $\sim 40\%$ lower than the present theoretical results for the C^{2+} ions in curve B. In principle, the dynamics of the double ionization is a very complicated process. At the present level of work on double ionization, it is not

Table 3
Partial ionization cross-sections (PICS, in cm^2) for CO_2

E (eV)	CO_2^+ ($\times 10^{-16}$)	CO^+ ($\times 10^{-17}$)	O^+ ($\times 10^{-17}$)	C^+ ($\times 10^{-17}$)	CO_2^{2+} ($\times 10^{-18}$)	C^{2+} ($\times 10^{-19}$)
20	0.37					
30	1.64	0.18	0.80	0.17		
40	2.54	0.89	0.95	0.48		
50	3.00	0.97	1.20	0.85	0.25	
60	3.24	1.25	1.31	1.18	0.60	
70	3.34	1.46	1.60	1.20	1.52	
80	3.36	1.64	1.78	1.47	1.95	0.4
90	3.33	1.83	1.90	1.69	2.24	1.8
100	3.24	1.90	2.40	1.26	3.10	2.3
150	2.87	2.22	2.60	1.47	3.02	3.0
200	2.61	2.10	2.70	1.40	2.95	4.2
250	2.18	1.85	2.55	1.31	2.65	3.9
300	2.01	1.60	2.50	1.23	2.25	3.7
400	1.65	1.50	2.30	1.15	1.92	3.5
500	1.38	1.41	1.65	1.10	1.50	3.4
800	0.97	1.09	1.40	0.87	1.11	2.3
1000	0.93	0.88	1.20	0.69	0.80	1.7
2000	0.52	0.67	1.00	0.55	0.72	1.4
5000	0.24	0.57	0.32	0.33	0.33	1.0
8000	0.15	0.25	0.15	0.15	0.16	0.4

possible to distinguish whether the process is direct or proceeds via correlation between the electrons. In fact, it is well known that the correlation between two target electrons is responsible for double electroionization. In the case of electron impact, outer-shell double ionization can be envisaged either as a first-order process (shake-off mechanism) or a second-order process (two-step mechanism). In general, the contribution of the shake-off process in double ionization is 3 times larger than the two-step mechanism [4].

In case of PICS, especially for dissociative processes, there is a confusing situation about the experimental data, as we note that the experimental data points [9] are not in satisfactory agreement with the theoretical results as well as many of the experimental data. The reason for the discrepancy has already been discussed [18]. The experimental data [9,11] show confusing results for the dissociative ionization processes. This may be due to systematic errors in their experiments and the different modes of normalization of their data. Furthermore, the experimental analysis of Crowe and McConkey [9] did not include the formation of minor ions via metastable states. Besides, the absolute data [13] show a significant disagreement with our results for dissociative ionization as well as other experimental data, whereas, in the case of the H_2 molecule [27,28], an excellent agreement within 5% uncertainty has been noticed [29]. The data of Straub et al. [13] are absolute with a statistical error of 4–10.5% for the dissociative ionization of CO_2; however, there may be some systematic error in the collection of minor ions produced via dissociative processes in their experiment. The accuracy of the present formula is linked with the accuracy of the oscillator strength. Theoretically, the accuracy of the present calculations can be increased if we have the more accurate experimental data for the photoionization cross-sections for the production of various ions.

4. Conclusions

We have provided semi-empirical results for PDDCS, PSDCS and the PICS for the production of CO_2^+ and CO_2^{2+} through direct O^+, CO^+, C^+ and C^{2+} through the dissociative electron ionization of

CO_2. In the absence of any data for partial differential cross-sections, the theory could provide the qualitative results for total differential cross-sections in comparison to the experimental data [14–16]. On the other hand, the PICS are found to be in good agreement with all the experimental data except the recent data [13], the disagreement with which is not understood explicitly. In all the ionization processes, the theoretical results predict the clear appearance of the threshold behavior of the cross-sections. Undoubtedly, the present results may be useful in plasma processes, astrochemistry and fusion research. Hence, all these investigations also support the successfulness of the semi-empirical approach in the calculation of partial differential cross-sections for molecules.

Acknowledgements

The author is thankful to University Grants Commission, India, for providing the financial assistance with contact grant Nos. F.7-26/97(NR) and F.9-11/98 (NR).

References

[1] R. Locht, M. Davister, Int. J. Mass Spectrom. Ion Process. 144 (1995) 105, and references therein.
[2] T.D. Märk, in: T.D. Märk, G.H. Dunn (Eds.), Electron Impact Ionisation, Springer, New York, 1985, and references therein.
[3] C.A. Barth, C.W. Hord, A.I. Stewart, A.L. Lane, Science 175 (1972) 309.
[4] A. Lahamam-Bennani, A. Duguet, in: S.P. Khare, D. Raj, A. Kumar (Eds.), Proceedings of the Tenth National Conference on Atomic and Molecular Physics, Meerut, 1997.
[5] J. Gomet, Thèse, Université de Rennes, Rennes, 1977.
[6] J. Peresse, F. Tuffin, Methodes Phys. Anal. 3 (1967) .
[7] B. Adamczyk, A.J.H. Boerboom, M. Lukasiewicz, Int. J. Mass Spectrom. Ion Phys. 9 (1972) 407.
[8] T.D. Märk, E. Hille, J. Chem. Phys. 69 (1978) 2492.
[9] A. Crowe, J.W. McConkey, J. Phys. B 7 (1974) 349.
[10] E. Krishnakumar, Int. J. Mass Spectrom. Ion Process. 97 (1990) 283.
[11] O.J. Orient, S.K. Srivastava, J. Phys. B 20 (1987) 3923.
[12] R.S. Freund, R.C. Wetzel, R.J. Shul, Phys. Rev. A 41 (1990) 5861.
[13] H.C. Straub, B.G. Lindsay, K.A. Smith, R.F. Stebbings, J. Chem. Phys. 105 (1996) 4015.
[14] T.W. Shyn, W.E. Sharp, Phys. Rev. A 20 (1979) 2332.
[15] G.N. Ogurtsov, J. Phys. B 31 (1998) 1805.
[16] C.B. Opal, E.C. Beaty, W.K. Peterson, At. Data Table 4 (1979) 209.
[17] D.K. Jain, S.P. Khare, J. Phys. B 9 (1976) 1429.
[18] S. Pal, S. Prakash, Rapid Commun. Mass Spectrom. 12 (1998) 297.
[19] S. Pal, S. Prakash, S. Kumar, Int. J. Mass Spectrom. Ion Process. 153 (1996) 79.
[20] S. Pal, S. Prakash, S. Kumar, Int. J. Mass Spectrom. Ion Process. 164 (1997) 14.
[21] S. Pal, S. Prakash, S. Kumar, Int. J. Mass Spectrom. Ion Process. 175 (1998) 247.
[22] E.N. Lassettre, A. Skerbele, M.A. Dillon, J. Chem. Phys. 50 (1967) 2829.
[23] J.W. Gallaghar, C.E. Brion, J.A.R. Samson, P.W. Langhoff, JILLA Data Rep. 32, Boulder, CO, 1987.
[24] T. Masuoka, Phys. Rev. A 50 (1994) 3886.
[25] G.D. Zeiss, W.J. Meath, J.C.F. MacDonald, D.J. Dawson, Can. J. Phys. 55 (1977) 2080.
[26] F.F. Rieke, W. Prepejchal, Phys. Rev. A 6 (1972) 1507.
[27] H.C. Straub, B.G. Lindsay, K.A. Smith, R.F. Stebbings, J. Chem. Phys. 105 (1996) 4015.
[28] H.C. Straub, B.G. Lindsay, K.A. Smith, R.F. Stebbings, Phys. Rev. A 54 (1996) 2146.
[29] S. Pal, S. Prakash, S. Kumar, J. Mass Spectrom. (1999, communicated).